

Research Article

Differences in the Hemolytic Behavior of Two Isomers in *Ophiopogon japonicus* *In Vitro* and *In Vivo* and Their Risk Warnings

Huan-Hua Xu ^{1,2}, Zhen-Hong Jiang,³ Yu-Ting Sun,² Li-Zhen Qiu,^{1,2} Long-Long Xu,^{2,4} Xiang-Lin Tang,² Zeng-Chun Ma,² and Yue Gao ^{1,2}

¹Tianjin University of Traditional Chinese Medicine, Tianjin 300193, China

²Department of Pharmaceutical Sciences, Beijing Institute of Radiation Medicine, Beijing 100850, China

³Jiangxi Province Key Laboratory of Molecular Medicine, Nanchang 330006, China

⁴College of Life Science and Bioengineering, Beijing University of Technology, Beijing 100124, China

Correspondence should be addressed to Yue Gao; gaoyue@bmi.ac.cn

Received 21 September 2020; Revised 25 November 2020; Accepted 2 December 2020; Published 15 December 2020

Academic Editor: Si Qin

Copyright © 2020 Huan-Hua Xu et al. This is an open access article distributed under the Creative Commons Attribution License, which permits unrestricted use, distribution, and reproduction in any medium, provided the original work is properly cited.

Ophiopogonin D (OPD) and Ophiopogonin D' (OPD') are two bioactive ingredients in *Ophiopogon japonicus*. Previously published studies have often focused on the therapeutic effects related to OPD's antioxidant capacity but underestimated the cytotoxicity-related side effects of OPD', which may result in unpredictable risks. In this study, we reported another side effect of OPD', hemolysis, and what was unexpected was that this side effect also appeared with OPD. Although hemolysis effects for saponins are familiar to researchers, the hemolytic behavior of OPD or OPD' and the interactions between these two isomers are unique. Therefore, we investigated the effects of OPD and OPD' alone or in combination on the hemolytic behavior *in vitro* and *in vivo* and adopted chemical compatibility and proteomics methods to explain the potential mechanism. Meanwhile, to explain the drug-drug interactions (DDIs), molecular modeling was applied to explore the possible common targets. In this study, we reported that OPD' caused hemolysis both *in vitro* and *in vivo*, while OPD only caused hemolysis *in vivo*. We clarified the differences and DDIs in the hemolytic behavior of the two isomers. An analysis of the underlying mechanism governing this phenomenon showed that hemolysis caused by OPD or OPD' was related to the destruction of the redox balance of erythrocytes. *In vivo*, in addition to the redox imbalance, the proteomics data demonstrated that lipid metabolic disorders and mitochondrial energy metabolism are extensively involved by hemolysis. We provided a comprehensive description of the hemolysis of two isomers in *Ophiopogon japonicus*, and risk warnings related to hemolysis were presented. Our research also provided a positive reference for the development and further research of such bioactive components.

1. Introduction

Hemolysis is the rupturing of erythrocytes and the release of their contents into the surrounding fluid. Hemolysis may occur *in vivo* or *in vitro*. Many factors can cause hemolysis, such as intrinsic causes (i.e., defects in the red blood cell (RBC) membrane, defects in hemoglobin [1], defective erythrocyte metabolism [2], Marchiafava-Micheli syndrome [3], etc.) and extrinsic causes (i.e., immune-mediated causes [4], toxicants or chemical reagents, phys-

ical factors [5], etc.). Regardless of intrinsic or extrinsic causes, disrupted redox balance is one of the common causes of hemolysis. The RBCs, in addition to their primary role as oxygen carriers, function as redox modulators [6]. However, this modulation ability is limited. Instead, mature erythrocytes, with their absence of protein synthesis and high oxygen-carrying capacity, are particularly susceptible to oxidative damage because they are rich in heme iron and oxygen, which can spontaneously generate H₂O₂ and lipid peroxides [7, 8].

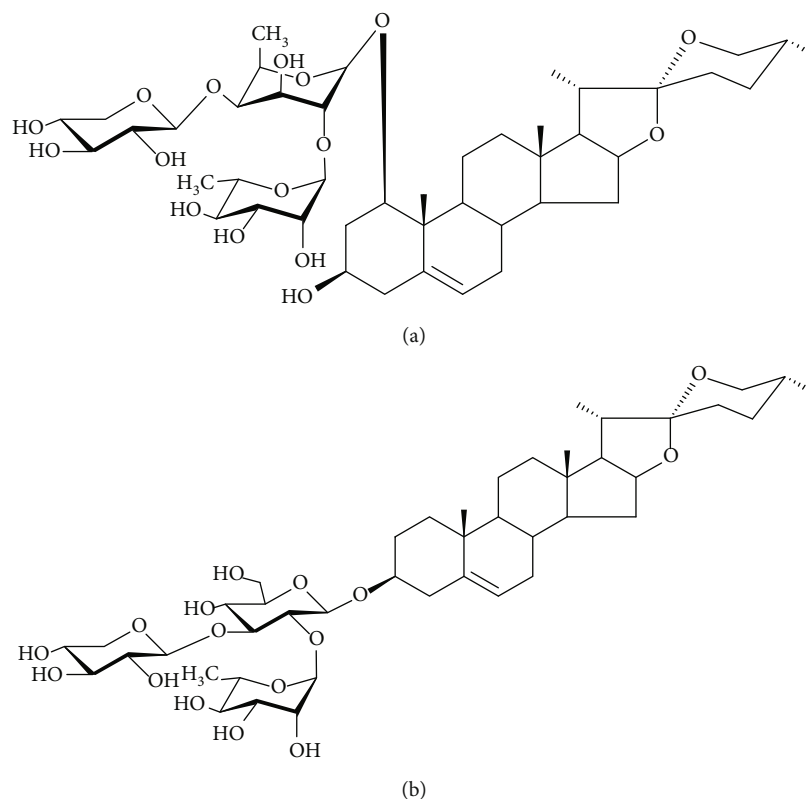


FIGURE 1: The chemical structure of Ophiopogonin D (OPD) and Ophiopogonin D' (OPD'). (a) Ophiopogonin D: ruscogenin 3-O- $\{\alpha$ -L-rhamnopyranosyl (1 \rightarrow 2)- $\{\beta$ -D-xylopyranosyl (1 \rightarrow 3)- β -D-fucopyranoside}. (b) Ophiopogonin D': diosgenin 3-O- $\{\alpha$ -L-rhamnopyranosyl (1 \rightarrow 2)- $\{\beta$ -D-xylopyranosyl (1 \rightarrow 3)- β -D-glucopyranoside}. Chemical formula: $C_{44}H_{70}O_{16}$, MW = 854.

Ophiopogon japonicus (Thunb.) is a well-known traditional Chinese medicine used to treat cardiovascular and chronic inflammatory diseases [9, 10]. Although it is not included in the medicinal and food dual-use list announced by the National Health Commission of the People's Republic of China, it is allowed to be used in functional foods [11], and in southern provinces of China, *Ophiopogon japonicus* is often used in dietary soups [12]. OPD and OPD' are two bioactive ingredients in *Ophiopogon japonicus*, and they are isomers of each other (see Figure 1). Previously, published literature on the active monomers in *Ophiopogon japonicus* mostly focused on OPD and its antioxidant effect [13–16]. Since 2017, the literature related to OPD' has gradually increased and is almost all related to its cytotoxicity [17]. Our mentor's team reported for the first time that OPD' at a concentration greater than $5 \mu\text{mol/L}$ can promote H9C2 cell apoptosis through the endoplasmic reticulum stress pathway [18]. Based on its cytotoxic effect, Zongliang et al. [19, 20] developed it as a potential antiproliferative cancer agent. However, with the deepening of our studies, we found that the cytotoxicity or other properties, such as the hemolytic properties that we discovered and reported in this manuscript, of OPD' limit its druggability. Moreover, in this manuscript, we reported that OPD, as an antioxidant, could also cause hemolysis *in vivo*. Despite extensive studies, a comprehensive analysis of hemolysis and drug-drug interactions (DDIs) between OPD and OPD' is missing, limiting our abil-

ity to assess the risks of medicines, functional foods, and diets containing *Ophiopogon japonicus*. Previous profiling studies lacked hemolysis, which necessarily underestimates its adverse effect and restricts analysis in a hemolysis-biased manner.

In this study, we investigated the effects of OPD and OPD' alone or in combination on the hemolytic behavior *in vitro* and *in vivo*. We identified that there is a huge difference in the hemolysis behavior between OPD and OPD' and clarified the specific manifestations of the behavior. We further adopted chemical compatibility and multiomics (i.e., metabolomics, lipidomics, and proteomics) methods to explain the different hemolytic behaviors *in vitro* and *in vivo*, and we found that both *in vitro* and *in vivo*, redox imbalance and lipid metabolism disorders played an important role in the hemolysis process. We also inferred that the DDIs between OPD and OPD' are not limited to the complementarity of physical and chemical properties, and a competitive target related to hemolysis may also exist. Therefore, molecular modeling technology was used to find the common target of the two isomers.

2. Materials and Methods

2.1. Drugs and Reagents. OPD (F05975, purity: 98% by HPLC) and OPD' (F581298, purity: 98% by HPLC) were purchased from the Shanghai EFE Biotechnology Co., Ltd. (Shanghai, China). Streptavidin PE conjugate (12-4317-87)

was purchased from Thermo Fisher. Biotinamido hexanoic acid N-hydroxysuccinimide ester (B2643, purity $\geq 98\%$, powder) was purchased from Sigma-Aldrich. 1,1-Diphenyl-2-trinitrophenylhydrazine (DPPH) was purchased from the Tokyo Chemical Industry Co., Ltd. (batch number: 217-591-8). Trolox (Lot No.1218C026, purity: not less than 50%) was purchased from the Solarbio Co., Ltd. (Beijing, China). Water was prepared by double distillation. All other reagents were of analytical or HPLC grade. Water, methanol, acetonitrile, and formic acid were purchased from the Sino-pharm Chemical Reagent Co., Ltd. (Beijing, China) and CNW Technologies GmbH (Düsseldorf, Germany).

2.2. Animals, Animal Management, and Experimental Design. The erythrocyte suspensions used in the *in vitro* hemolysis test were collected from New Zealand white rabbits purchased from the Beijing Jinmuyang Laboratory Animal Breeding Co., Ltd. (production license: SCXK (Jing)-2015-0005). An *in vivo* hemolysis study was conducted in apparently healthy adult KM mice (18-20 g, male). Animals were purchased from the Beijing Keyu Animal Breeding Center (production license: SCXK (Jing)-2018-0010). The animals used in the multiomics research were Wistar rats that were purchased from the Beijing Vital River Laboratory Animal Technology Co. Ltd. (production license: SCXK (Jing)-2016-0011). All animals were housed in an environmentally controlled breeding room (temperature: $22 \pm 2^\circ\text{C}$, humidity: $50 \pm 5\%$, dark/light cycle: 12/12 h). The animals were provided with standard laboratory food and water. The rabbits were raised in a single cage, and 3 mice and rats were raised per cage. During the experiment, the animals had free access to food and water [21, 22]. The experimental protocols were approved by the Animal Ethics Committee of Academy of Military Medical Sciences (approval No. IACUC-DWZX-2020-684) and were performed in accordance with the guidelines of the National Institutes of Health for the Care and Use of Laboratory Animals. Prior to each experiment, all animals were kept under laboratory conditions for a period of 4 days or more for acclimatization. Since there are multiple independent animal experiments, the experimental design is described in detail under their respective experimental items, such as in Sections 2.3, 2.6, and 2.7.

2.3. In Vitro Hemolysis Test. The *in vitro* hemolysis test referred to the “Technical Guidelines for the Study of Stimulating and Hemolytic Properties of Traditional Chinese Medicines and Natural Medicines” issued by the State Food and Drug Administration in 2005 (Guideline number: [Z]-GPT4-1). Four groups were designed to investigate whether OPD and OPD' exhibit drug-drug interactions in hemolytic behavior. They were the OPD group, OPD' group, OPD+OPD' group (premixed before administration), and OPD \rightarrow OPD' group (based on the isomers' physical and chemical properties, considering whether preadministration has a protective effect, we set the OPD \rightarrow OPD' group, in which OPD and OPD' were used in sequence, 5 min apart). The concentrations of OPD and OPD' in each group were 0, 5, 10, 20, and 40 $\mu\text{g}/\text{mL}$. After each group of samples were prepared

according to the guidelines, they were immediately placed in a $37 \pm 0.5^\circ\text{C}$ water bath for 3 h, removed, and centrifuged at 3000 rpm for 5 min, and the supernatant was transferred to a 24-well plate. An ultraviolet spectrophotometer was used to measure the absorbance of each group of samples at 570 nm, calculate the hemolysis rate, and draw the hemolysis rate-concentration curve.

One of the difficulties in the study of active monomers of traditional Chinese medicine is poor water solubility, resulting in dose deviation and inaccurate concentration. Both of OPD and OPD' suffered from this problem, and our pilot studies have shown that 25% methanol in saline as the solvent can not only completely dissolve OPD and OPD' but is also safe for RBCs within 4 h of *in vitro* hemolysis experiments. Compared with other solvents, there were no dose deviations, and the results were extrapolated to be more credible clinically.

2.4. Effects of Different Solvents or Compatible Drugs on the Hemolytic Behavior of OPD'. To investigate the effects of commonly used clinical solvents on OPD' hemolytic behavior, saline, glucose (5%), fructose (10%), and mannitol (20%) were selected to dilute the OPD' stock liquid, in which OPD' was completely dissolved in methanol (25%), to the following series of concentrations 5, 10, 20, 40, and 80 $\mu\text{g}/\text{mL}$. The hemolysis rate of each sample was determined according to the guidelines, and the hemolysis rate-concentration curve was drawn.

Trolox is a reductive water-soluble vitamin E that protects RBCs from hemolysis due to its oxidative properties. Investigating the effect of the combined use of Trolox and OPD' on the hemolytic behavior of OPD' was helpful to explore the reasons for the difference in the hemolytic behavior of the two isomers *in vitro*. OPD' (40 $\mu\text{g}/\text{mL}$) was selected as the positive control; at this concentration, the hemolysis rate of RBCs *in vitro* was almost 100%. The concentration of OPD' was fixed and mixed with different concentrations of Trolox solution, and then, the relationship between the change in the hemolysis rate and the concentration of Trolox was revealed. In addition, in the *in vitro* hemolysis test, we discovered that the OPD \rightarrow OPD' group also exhibited drug-drug interactions. Here, we applied the same procedure as with Trolox to further explore the effect of OPD on OPD'-induced hemolysis.

2.5. Reasonable Explanation of the Different Hemolytic Behaviors of OPD' and OPD In Vitro

2.5.1. DPPH Method for the Determination of the Antioxidizability of OPD and OPD'. The DPPH method [23] was first proposed in 1958 and can be used to determine the antioxidant capacity of biological samples *in vitro*. In this study, it was used to investigate whether the difference in the hemolytic behavior between the two isomers is related to the oxidizability and reducibility.

2 mL of 5, 10, 20, and 40 $\mu\text{g}/\text{mL}$ OPD and OPD' samples was added to 5 tubes, followed by the addition of 4 mL of 24 mg/L DPPH ethanol (95%) solution under dark

conditions and shaking. After avoiding light at room temperature for 30 min, UV-visible spectrophotometry was used to measure the absorbance (A_i) at 517 nm. The same amount of DPPH ethanol (95%) without sample extract was used as the control group, and the absorbance (A_0) of the control group was measured by the same method. Equation (1) was used to calculate the inhibition rate, which represents the antioxidant capacity, and the greater the inhibition rate, the stronger the antioxidant capacity.

$$\text{Inhibition rate} = \frac{A_0 - A_i}{A_0} \times 100\%. \quad (1)$$

2.5.2. Effect of OPD' Alone or in Combination with OPD on the SOD, MDA, LDH, GSH, and Na⁺-K⁺-ATPase Content. The experiment was divided into 3 groups: normal control group (NC), OPD' group, and OPD→OPD' group (OPD and OPD' were used in sequence 5 min apart). To a 10 mL test tube, 2.5 mL of RBC suspension (20%) and then 2.5 mL of test drugs in different groups were added in turn, with the same volume of solvent added for the control in the NC group. After careful mixing, the mixture was placed in a 37°C constant temperature water bath and incubated for 4 h. After incubation, the test tubes were carefully removed and centrifuged at 1500 rpm (4°C) for 10 min. The supernatant was discarded with a disposable pipette, and 0.2 mL of the lower layer of the RBC pellet was taken for counting cells, to which 3 mL of prechilled purified water was added, followed by mixing and shaking to fully lyse the RBCs. Then, it was stored at 4°C until use. The ELISA kit instructions were followed to determine lactate dehydrogenase (LDH) enzyme activity and the contents of malondialdehyde (MDA), superoxide dismutase (SOD), glutathione (GSH), and Na⁺-K⁺-ATPase in the cytoplasm of each group of erythrocytes [24, 25].

2.6. In Vivo Hemolysis Test. Biotin labeling, as an alternative nonradioactive approach for the determination of RBC survival, is widely accepted [26, 27]. In this study, 30 mg/kg biotinamidohexanoic acid N-hydroxysuccinimide ester solution was injected via the tail vein to label RBCs. After 1 h, to determine the efficiency of biotin labeling, blood samples were collected from each animal, and streptavidin PE conjugate was used to bind biotin, which was used to label RBCs for flow cytometric analysis. Animals with a labeling efficiency greater than or equal to 95% were selected for RBC lifespan analysis.

Fifteen mice were randomly assigned to 3 groups: normal control group (NC), OPD group, and OPD' group. According to the limit of the clinical hemolysis rate (5%) and the results obtained from the *in vitro* hemolysis test, the plasma concentration of OPD' should not exceed 5 µg/mL. The doses of OPD and OPD' in each group were defined as 0.25 mg/kg; at this dose, the configuration of the drug was free of organic reagents. All drugs were administered by intravascular injection for 30 days. Changes in the percentage of labeled RBCs with the administration time can be used to estimate the RBC lifespan. The first blood sample analysis

should be completed within 3 days after administration, and the subsequent analysis interval was based on the first analysis results, but did not exceed 7 days.

2.7. Proteomics Methods to Explore the Potential Mechanism of OPD- and OPD'-Induced Hemolysis In Vivo. Twenty-two rats were randomly assigned to 3 groups: the normal control group (NC, $n = 6$), OPD group ($n = 8$), and OPD' group ($n = 8$). All drugs were administered by intravascular injection for 14 days. According to the limit of the clinical hemolysis rate (5%) and the results obtained from the *in vitro* hemolysis test, the doses of OPD and OPD' in each group were defined as 0.25 mg/kg. Plasma was prepared by centrifugation for metabolomics and lipidomics analysis. Both metabolomics and lipidomics analyses were performed on a UPLC-MS/MS system tandem with different mass spectrometers and separated under different LC conditions (unpublished manuscript).

At the same time, the nonanticoagulated whole blood of each group was prepared into RBC suspensions according to the guidelines (Guideline number: [Z]-GPT4-1). Subsequently, pure water was added to fully lyse the RBC membrane, followed by centrifugation. The supernatant was discarded, and the precipitate was washed 2-3 times repeatedly. Then, the precipitate was the prepared blood ghost, i.e., the RBC membrane. Fifty microliters of sample lysate was added, and then, protease inhibitor PMSF was added to make the final concentration 1 mM. The solution was then boiled for 10 min and centrifuged at 12000 g for 10 min at room temperature. The supernatant was centrifuged again, and the supernatant is the total protein solution of the sample, with the protein concentration determined by the BCA method. After protein quantification, 100 µg of each sample was placed into a 10 K ultrafiltration tube, and the filter-aided sample preparation (FASP) method [28] was used to enzymatically digest the protein. For tandem mass tag (TMT) labeling, 41 µL of anhydrous acetonitrile was added to a TMT⁶ [29] reagent vial at room temperature. The reagents were dissolved for 5 min and centrifuged. Then, 41 µL of the TMT⁶ label reagent was added to each 100 µL sample for mixing. The tubes were incubated at room temperature for 1 h. Finally, 8 µL of 5% hydroxylamine was added to each sample and incubated for 15 min to terminate the reaction. The prepared sample was first separated by reverse-phase chromatographic separation, and the sample in the period of 8-60 min was collected. Then, the collected samples were further separated by a HPLC system and detected by mass spectrometry. The data were analyzed by Proteome Discoverer™ software (Version 2.2, Thermo, USA), and the databases utilized were UniProt-proteome_UP000002494-Rattus norvegicus (Rat) (Strain Brown Norway). Detailed proteomic analysis methods can be seen in the supplementary materials (see Method S1).

2.8. Molecular Modeling to Find the Common Hemolysis Target of OPD and OPD'. The bioassay of OPD' and OPD indicates that they will result in hemolysis *in vitro* and *in vivo*. To predict the putative targets and conduct pathway enrichment analysis for OPD' and OPD, the targets

associated with hemolysis were collected from famous databases such as UniProt. Putative target prediction was based on the SEA (similarity ensemble approach) [30] approach. This method is based on the molecular fingerprint to calculate the similarity between the query molecule and the corresponding ligand molecule in the target database. ChEMBL17 was used as the target database. RDKit ECFP4 (1024 bits) was used as the molecular fingerprint. Pharmaceutical target seeker (PTS) [31] was used as a shape-based approach. In PTS, the weighted Gaussian algorithm (WEGA) [32], which is based on molecular three-dimensional conformation superposition, was used to calculate the 3D similarity between the query molecule and the corresponding ligand molecule in the target database. The Reactome Pathway Database (<https://reactome.org>) was used for pathway analysis for the predicted potential targets of OPD' and OPD.

2.9. Statistical Analysis. SAS version 9.1 (SAS Inc. USA) was used to perform the statistical analyses. All data are expressed as the mean \pm SD. For comparisons between two groups, Student's *t*-test was used. For comparisons among three or more groups, the data were analyzed using a one-way analysis of variance (ANOVA). For all analyses, a *p* value of <0.05 was considered to indicate statistical significance and a *p* value of <0.01 was considered to indicate extreme statistical significance. GraphPad Prism (version 6.0) was used to draw the statistical figures.

3. Results and Discussion

3.1. In Vitro Hemolytic Behavior of OPD and OPD' Is Inconsistent. The hemolytic behaviors of the 4 test groups (i.e., OPD, OPD', OPD \rightarrow OPD', and OPD+OPD') are presented in Figure 2. The curve shows that OPD has no erythrocyte hemolysis in the concentration range of 0-40 $\mu\text{g}/\text{mL}$. In contrast, the RBCs were rapidly hemolyzed within 15 min after the administration of OPD', and the hemolysis rate was linearly related to the concentration of OPD'. According to the clinical guidelines, the unacceptable hemolysis rate is 5% (Guideline number: [Z]-GPT4-1); therefore, the concentration of OPD' should not exceed 5 $\mu\text{g}/\text{mL}$. More interesting data came from the other two groups, and the hemolytic behavior of OPD' was weak when OPD and OPD' were used in sequence (group OPD \rightarrow OPD'). At a concentration of 20 $\mu\text{g}/\text{mL}$, the hemolysis rate of the OPD' group was approximately 10% lower than that of the OPD+OPD' group. However, the OPD \rightarrow OPD' group's data suggest that OPD plays a role in protecting erythrocytes from being destroyed by OPD'. Obviously, the hemolytic behavior of each group is inconsistent, which provides much evidence for subsequent research.

3.2. Different Solvents or Compatible Drugs Affect the Hemolytic Behavior of OPD' In Vitro. The research results have shown that different solvents or compatible drugs have a significant effect on OPD'-induced hemolysis. As shown in Figure 3(a), compared with saline, glucose (5%), fructose (10%), and mannitol (20%) alleviated hemolysis caused by

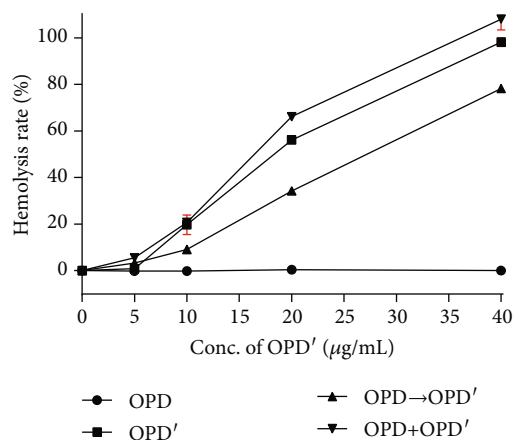


FIGURE 2: *In vitro* hemolytic behavior of OPD and OPD'. The error bars represent the standard deviation of measurements for 4 parallel samples in four separate groups ($n = 4$).

OPD', and mannitol (20%) had the most obvious alleviating effect. For example, when mannitol (20%) was used as the solvent, the hemolysis rate of OPD' (40 $\mu\text{g}/\text{mL}$) was $4.67\% \pm 0.42\%$, and this value was $98.15\% \pm 1.80\%$ when saline was used as the solvent; therefore, the hemolysis rates were reduced by 93.48%. Correspondingly, the hemolysis rates of glucose (5%) and fructose (10%) were $22.53\% \pm 1.26\%$ and $23.36\% \pm 1.07\%$, respectively.

As shown in Figure 3(b), the compatible drug Trolox did not cause hemolysis in a series of concentrations, and 40 $\mu\text{g}/\text{mL}$ OPD' maintained a hemolysis rate close to 100% ($98.15\% \pm 1.80\%$). When a series of concentrations of OPD and Trolox were pretreated with erythrocytes, the high hemolysis rate caused by OPD' (40 $\mu\text{g}/\text{mL}$) was decreased, and the degree of reduction was linearly related to the concentration of OPD and Trolox. In the range of 5-10 $\mu\text{g}/\text{mL}$, the decreasing effect of OPD was better than that of Trolox. However, in the range of 20-40 $\mu\text{g}/\text{mL}$, the decreasing effect of OPD was weakened compared with that of Trolox. The better the decreasing effect, the stronger the ability to protect erythrocytes.

3.3. Relationship between Different Hemolytic Behaviors of OPD and OPD' and the Redox Balance. According to the results of Figures 2 and 3, OPD, Trolox, glucose (5%), and fructose (10%) can all alleviate the hemolysis rate caused by OPD'. Among them, Trolox, glucose (5%), and fructose (10%) are all reductive substances. To explore whether the difference in the hemolysis behavior of OPD and OPD' is related to reductive or oxidative properties, the DPPH method was adopted. As shown in Figure 4, OPD' has almost no DPPH free radical scavenging ability. In contrast, the DPPH free radical scavenging ability of OPD became stronger as the concentration of OPD gradually increased. However, compared with the positive control drug Trolox, OPD is not as good as Trolox in scavenging DPPH free radicals. Therefore, OPD' has almost no reducibility, while OPD has a certain degree of reducibility, which could reasonably

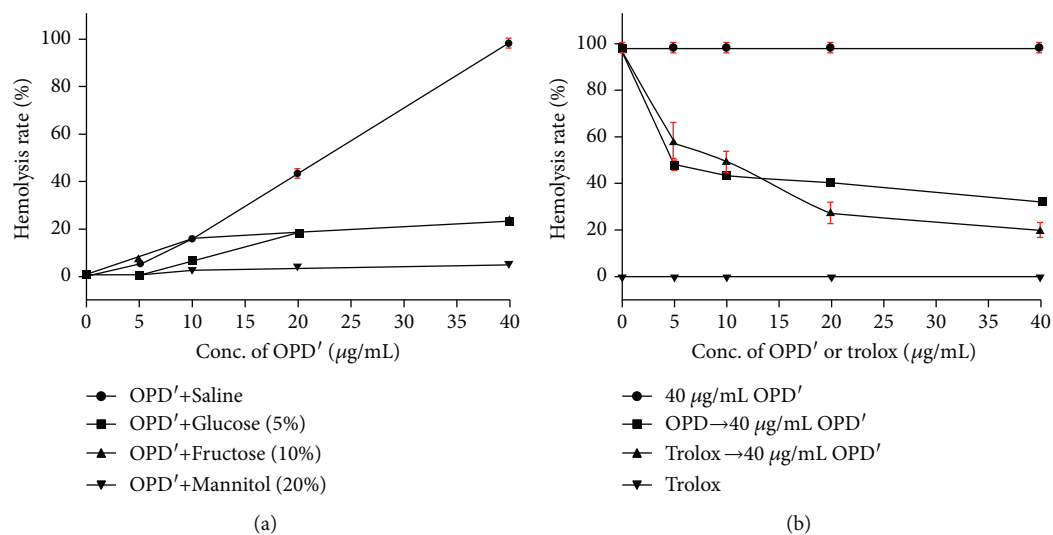


FIGURE 3: Effects of different solvents or compatible drugs on hemolytic behavior of OPD'. (a) The commonly used clinical solvents. (b) The compatible drugs, OPD, and Trolox. The error bars represent the standard deviation of measurements for 4 parallel samples in four separate groups ($n = 4$).

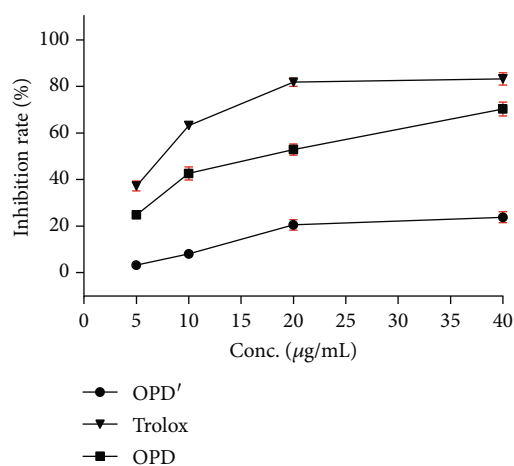


FIGURE 4: The scavenging ability of OPD, OPD', and Trolox in different concentrations on DPPH free radicals. The error bars represent the standard deviation of measurements for 4 parallel samples in three separate groups ($n = 4$).

explain why OPD has the ability to alleviate hemolysis caused by OPD' similar to Trolox, glucose (5%), and fructose (10%).

As shown in Figure 5(a), the LDH content in the erythrocyte cytoplasm gradually decreased as the OPD' concentration increased compared with that in the NC group. At concentrations of 10 µg/mL and 20 µg/mL, the difference was significant ($p < 0.05$), and at a concentration of 40 µg/mL, the difference was very significant ($p < 0.01$). When OPD was used to pretreat erythrocytes at a concentration of 40 µg/mL, the LDH content in the cytoplasm of erythrocytes increased significantly ($p < 0.05$) compared with that in the OPD single-use group. After treatment with OPD', the MDA content in the cytoplasm of RBCs increased, which was positively correlated with the OPD' concentration. Pretreat-

ment with OPD alleviated the increase in the MDA content caused by OPD' (Figure 5(b)). Trends similar to the change in the LDH content also appeared in the SOD, GSH, and $\text{Na}^+ - \text{K}^+ - \text{ATPase}$ content (Figures 5(c)–5(e)). After treatment with OPD', the contents of SOD, GSH, and $\text{Na}^+ - \text{K}^+ - \text{ATPase}$ in the erythrocyte cytoplasm all showed a dose-dependent decrease, and this decrease was reversed or alleviated by pretreatment with OPD to a certain extent.

From the results of the *in vitro* hemolysis test, the effects of solvents and compatible drugs on the hemolysis test, and the detection of redox balance-related factors, it is speculated that the hemolysis caused by OPD' *in vitro* may be related to the destruction of the redox balance. LDH is a marker enzyme that exists in the cytoplasm of cells and can sensitively reflect the degree of cell membrane damage [33]. MDA is a naturally occurring product of lipid peroxidation and prostaglandin biosynthesis that is mutagenic and carcinogenic [34], and the MDA content reflects the degree of lipid peroxidation in erythrocytes. SODs constitute a very important antioxidant defense against oxidative stress in the body [35]. The enzyme acts as a good therapeutic agent against reactive oxygen species-mediated diseases. GSH plays an important role in the body's biochemical defense system. In addition to eliminating free radicals generated by metabolism [36], GSH can also improve the body's immunity. Both SOD and GSH play a very important role in maintaining the redox balance. After treatment with OPD', the erythrocyte membrane was damaged, resulting in increased membrane permeability and the leakage of cell content such as LDH. The MDA content was significantly increased, and both the SOD and the GSH content were significantly decreased. $\text{Na}^+ - \text{K}^+ - \text{ATPase}$ is an important enzyme for erythrocytes to complete energy metabolism [37]. It actively transports K^+ and Na^+ , thereby maintaining the balance of osmotic pressure on both sides of the cell membrane. In our study, after treatment with OPD', its enzyme activity was suppressed.

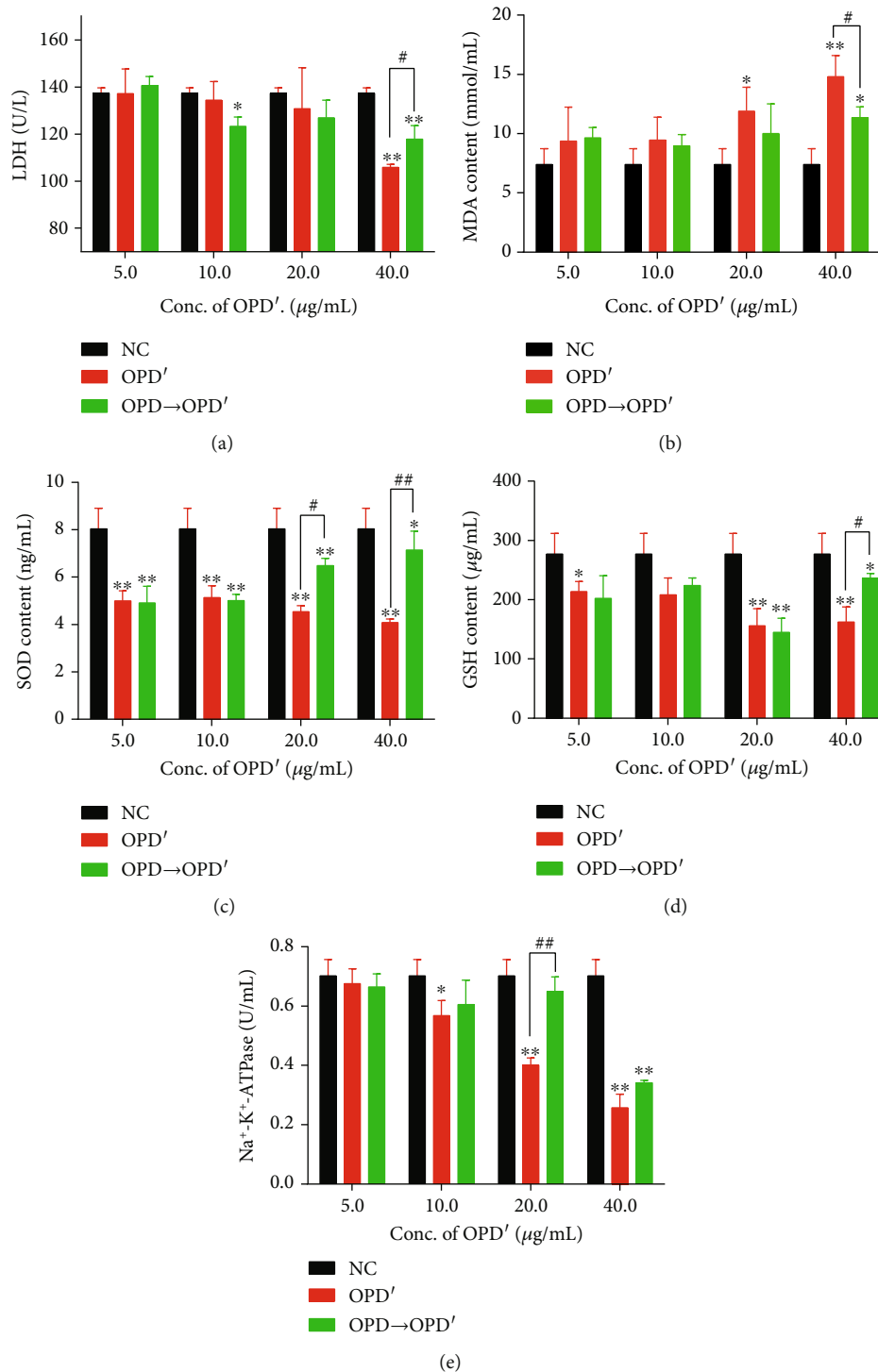


FIGURE 5: Effects of OPD' and OPD pretreated (OPD→OPD') on LDH, MDA, SOD, GSH, and Na⁺-K⁺-ATPase content: (a) LDH content, (b) MDA content, (c) SOD content, (d) GSH content, and (e) Na⁺-K⁺-ATPase content. The error bars represent the standard deviation of measurements for 3 parallel samples in three separate groups ($n = 3$). * Compared with the NC group, the statistical value was significant ($p < 0.05$); ** compared with the NC group, the statistical value was very significant ($p < 0.01$); # compared with the OPD' group, the statistical value was significant ($p < 0.05$); ## compared with the OPD' group, the statistical value was very significant ($p < 0.01$).

Therefore, based on the experimental results, we can infer that the hemolytic behavior of OPD' in RBCs manifests as oxidative damage. By inhibiting the activities of SOD and

GSH, it reduces the ability of RBCs to scavenge superoxide anion free radicals, leading to increased membrane permeability, aggravating the degree of lipid peroxidation of RBC

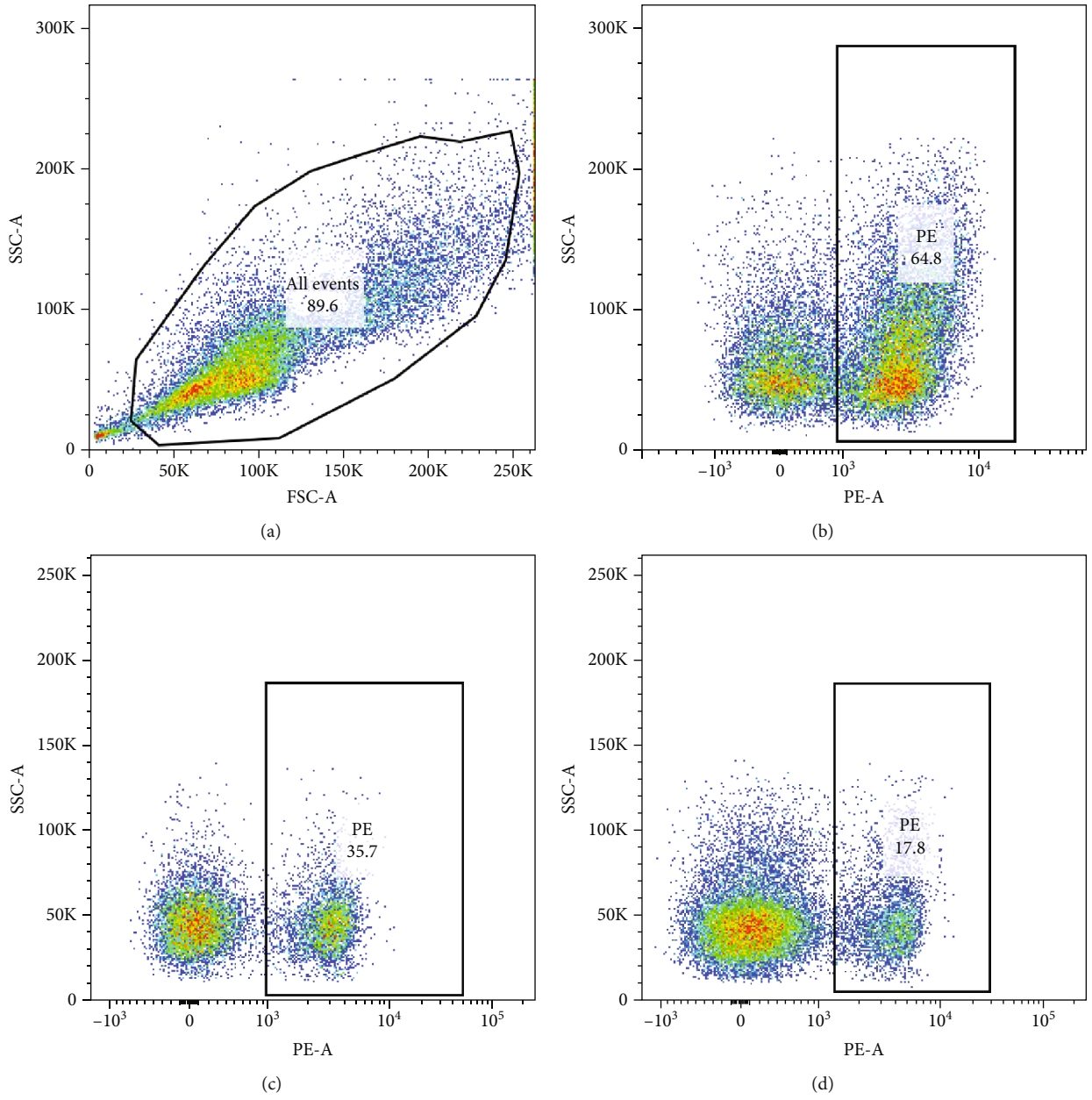


FIGURE 6: Continued.

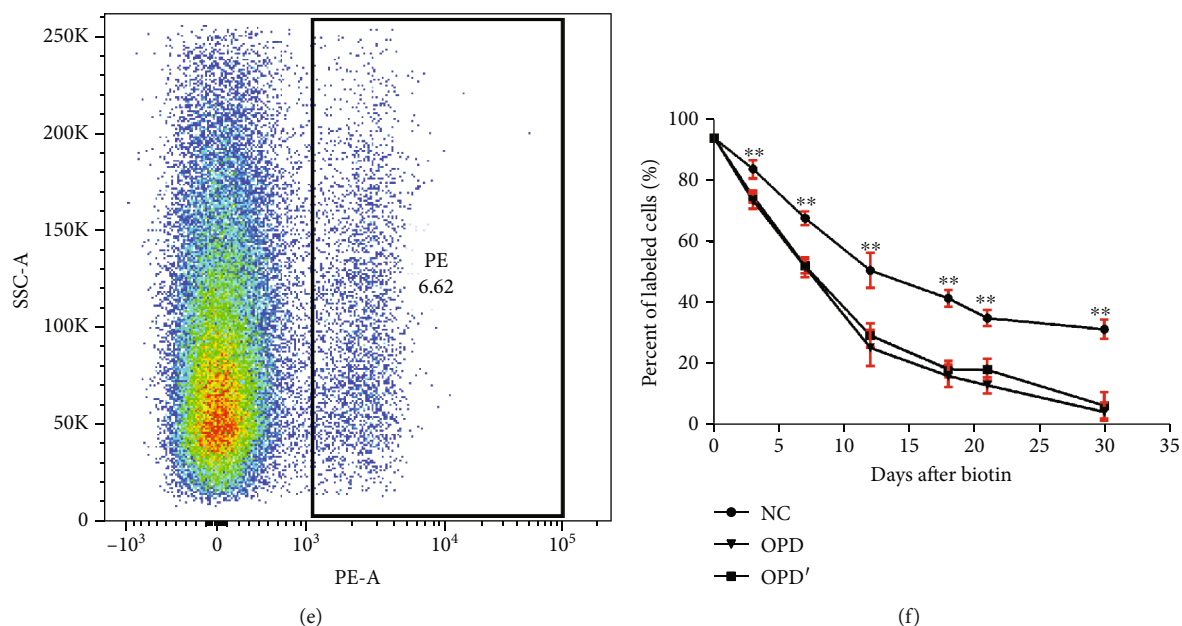


FIGURE 6: Effects of OPD' and OPD on erythrocyte life span. (a) and (b) exhibited the flow cytometry analysis workflow; (b) 7th day, NC group; (c) 12th day, OPD group; (d) 21th day, OPD group; (e) 30th day, OPD' group; (f) relationship between percent of labelled cells and days after biotin. The error bars represent the standard deviation of measurements for 5 parallel samples in three separate groups ($n = 5$). **Compared with the OPD and OPD' group, the statistical value was very significant ($p < 0.01$).

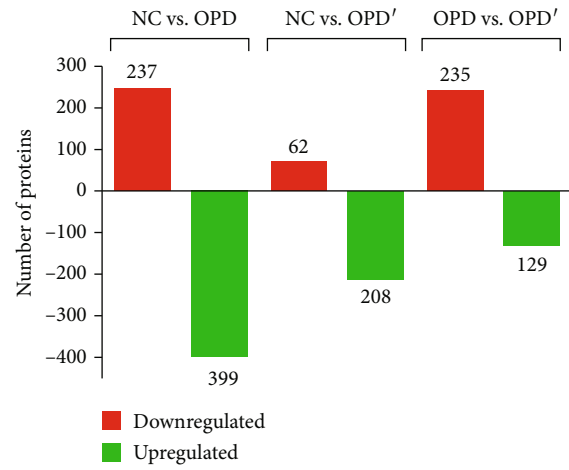
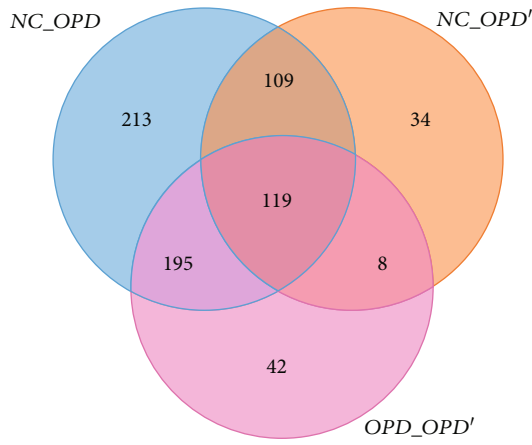
membranes, resulting in increased MDA content, and further aggravating the oxidative damage of cell membranes. Increased membrane permeability also induced LDH leakage, which resulted in a decreased LDH content in the cytoplasm of erythrocytes. OPD' can also inhibit the activity of ATPase on the RBC membrane, affect its material transport and energy metabolism, and lead to changes in the structure and function of the membrane. Eventually, erythrocytes were ruptured, and hemolysis occurred. However, OPD can reverse the hemolysis caused by OPD' to a certain extent because of its reducibility.

3.4. Both OPD and OPD' Caused Hemolysis In Vivo. The differences between the *in vitro* hemolysis behavior of OPD and OPD' and the drug-drug interactions (DDIs) based on the hemolysis behavior of the two isomers were very peculiar, which makes us eager to explore the hemolysis behavior and DDIs of these two isomers *in vivo*. We have used a variety of methods to study the hemolytic behavior of OPD and OPD' *in vivo*, such as single-dose- and multiple-dose-based acute toxicity tests (single-dose or 14 days) and subacute toxicity tests (30 days), and the experimental animals include rats and mice [38]. The data in unpublished manuscripts show that multiple doses of OPD and OPD' both caused hemolysis *in vivo*, which was manifested by a decrease in the HGB content, a decrease in the RBC count, and a significant increase in the absolute value and percentage of RET. Correspondingly, the results related to hemolysis were also observed in the pathological changes of organs and the animal body weight. Urine test results also indicate the occurrence of intravascular hemolysis.

Although these indicators indicate the occurrence of hemolysis, they are not the gold standard examination for the diagnosis of hemolysis. The essential feature of any hemolytic disorder is the shortened RBC lifespan [39, 40]. As shown in Figure 6(f), administering OPD and OPD' through tail vein injection for 30 consecutive days significantly shortens the lifespan of RBCs. At the same time point (i.e., 3rd, 7th, 12th, 18th, 21st, and 30th), compared with the NC group, the percentages of labeled cells in both the OPD and OPD' groups were significantly decreased ($p < 0.05$ or 0.01). These results confirmed that both OPD and OPD' caused hemolysis *in vivo*. Thus far, we not only discovered the hemolysis of OPD' *in vitro* but also found the hemolysis of OPD *in vivo*.

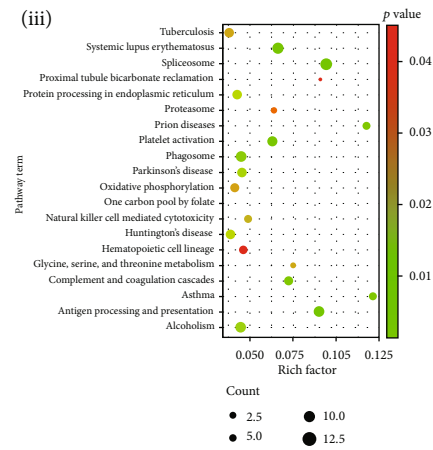
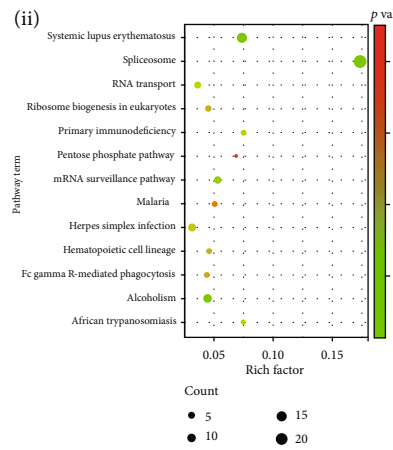
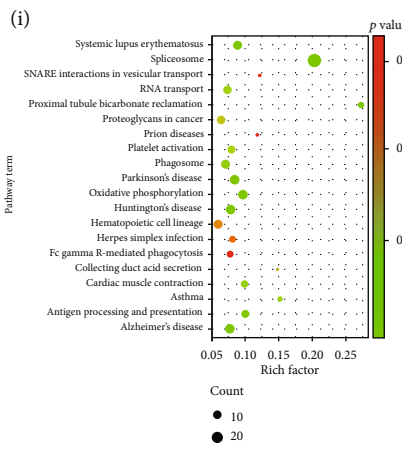
There are some possible speculations for this phenomenon; one is that OPD is biotransformed into OPD' or its analogues in animals, and the other one is that both OPD and OPD' were metabolized into more activated forms for hemolysis, but the speculations lack sufficient data. Based on the speculations, we studied the possibility of the conversion between OPD and OPD' at both the *in vivo* and *in vitro* levels, and the results did not find any signs of such conversion. We hypothesized that the inconsistency of the hemolytic behavior of OPD *in vivo* and *in vitro* may be related to its metabolites, and related research is ongoing.

3.5. Multiomics Studies Reveal the Underlying Mechanism of Hemolysis Caused by OPD and OPD'. Our previous results in an unpublished study demonstrated that changes in endogenous differential metabolites and differential lipids, enrichment of differential metabolic pathways, and



(a)

(b)



(c)

FIGURE 7: Continued.

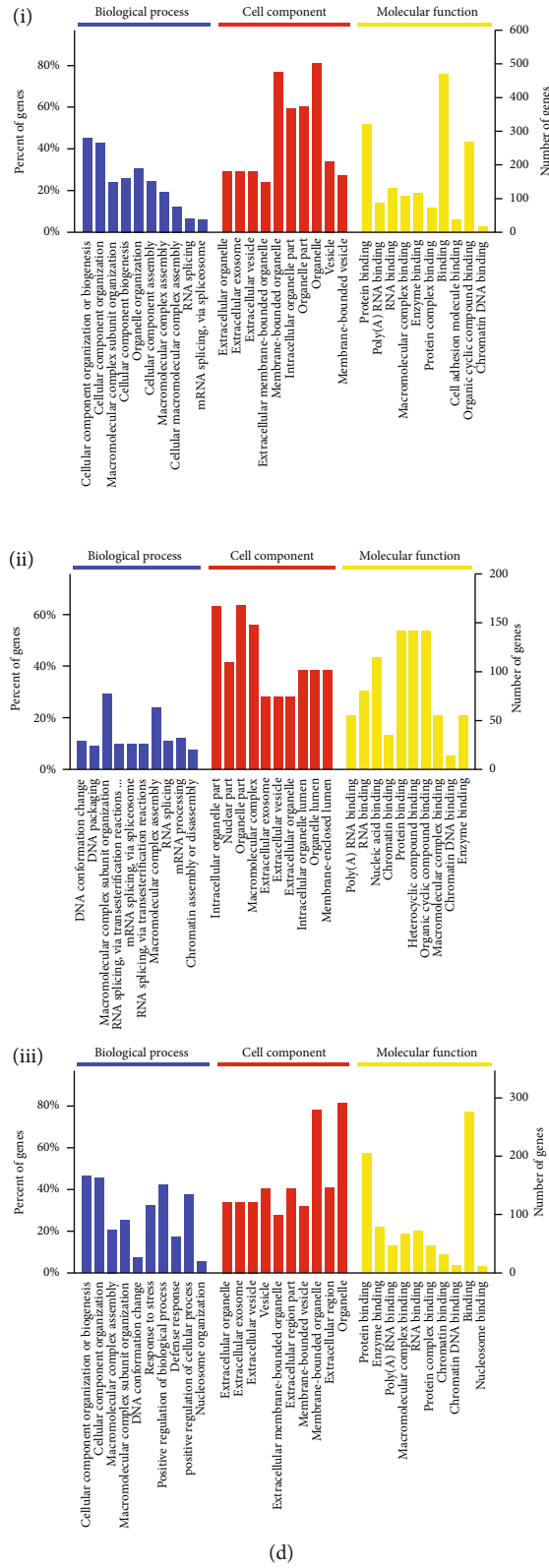


FIGURE 7: Continued.

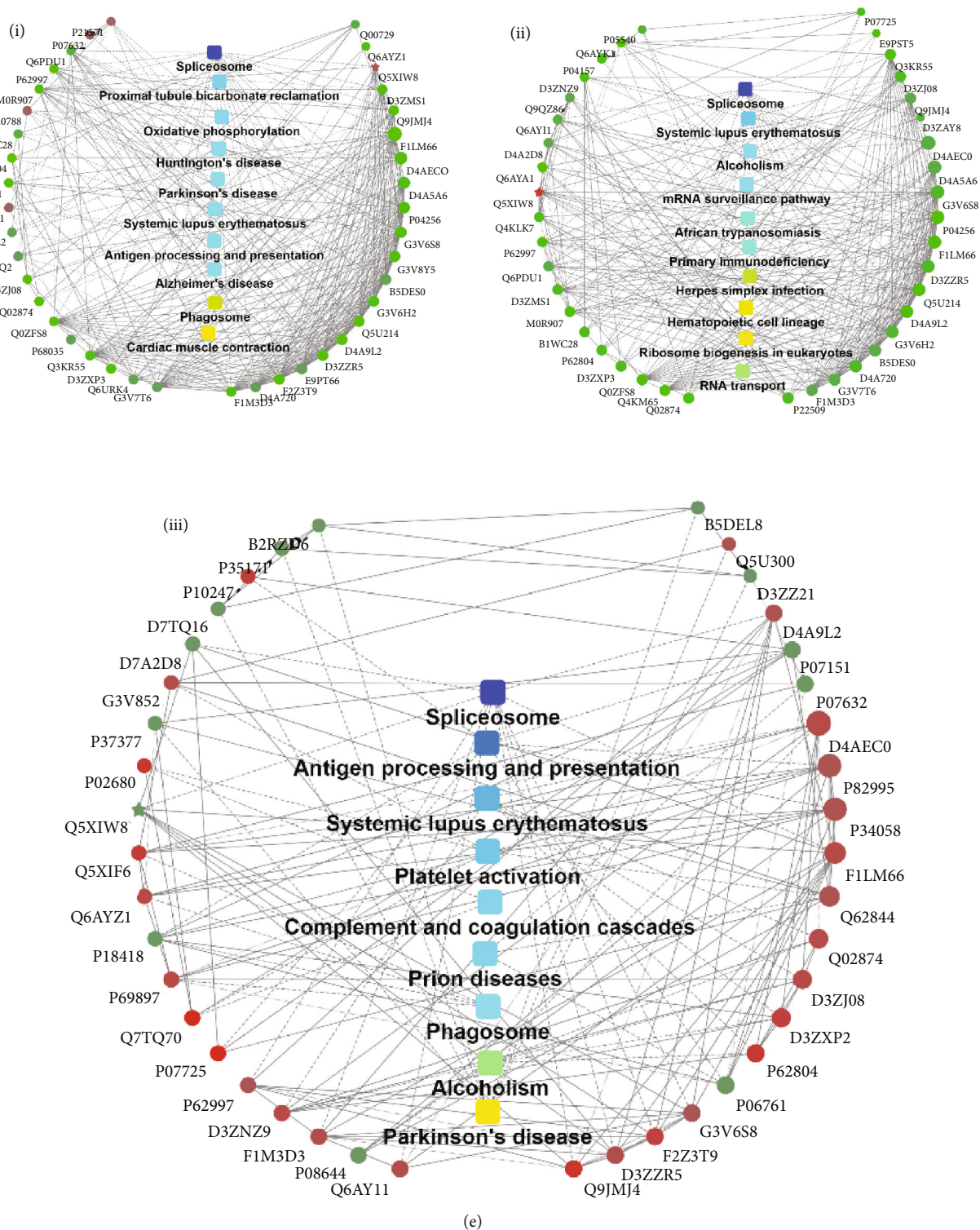


FIGURE 7: Proteomics results of OPD and OPD'. (a) Venn plot of three compared sets. (b) Up- or downregulated differential proteins in three compared sets. (c) KEGG bubble plot of three compared sets. (d) Top 10 biological processes, cell components, and molecular functions of three compared sets. (e) PPI network plots of three compared sets. (i) NC-OPD-compared group, (ii) NC-OPD'-compared group, and (iii) OPD-OPD'-compared group.

correlation analysis all showed that the causes of the hemolysis of OPD and OPD' are closely related to disorders of phospholipid metabolism.

In this study, we focused on the proteomics results of blood ghosts. Based on the screening criteria (i.e., fold-change > 1.5 or < 0.6), 2905 credible proteins were obtained.

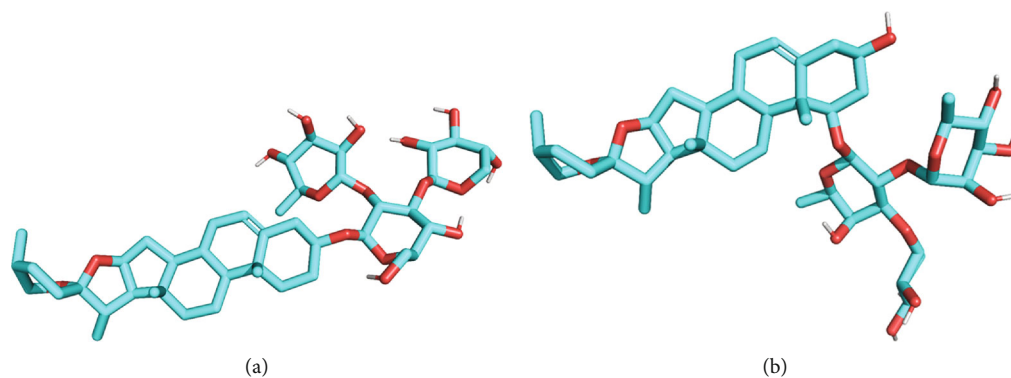


FIGURE 8: Three-dimensional molecular structures of OPD and OPD': (a) OPD'; (b) OPD.

Compared with the NC group, 636 and 270 proteins were differentially expressed between the OPD and OPD' groups, respectively, and 364 proteins were differentially expressed between the OPD and OPD' groups. As shown in Figure 7(a), a Venn plot shows the logical relationships between the three compared sets. In Figure 7(b), the number of up- or downregulated differential proteins is displayed. In Figure 7(c), a bubble plot of KEGG showed that the related enriched significant pathway terms resulted in three compared sets. In Figure 7(d), the top 10 biological processes, cell components, and molecular functions of the three compared sets are displayed. Under OPD intervention, blood ghost proteomics results suggested that biological processes were significantly enriched in the cellular component, subunit or organelle organization, biogenesis, and assembly. However, when treated with OPD', biological processes were different and enriched in DNA conformation changes and packaging, RNA splicing, mRNA splicing, and processing. This provides a new perspective for understanding the interactions of OPD' and OPD with RBCs. Cell component analysis indicated that extracellular organelles, exosomes, extracellular membrane-bound organelles, and vesicles were significantly changed in the NC vs. OPD comparison set. In the NC vs. OPD' comparison set, in addition to extracellular organelles, exosomes, and vesicles, intracellular organelle parts and lumens were significantly changed. At the molecular function level, OPD and OPD' were similar, and they were both enriched in enzyme, protein, and RNA binding. To realize these analyses and visualize the protein interactions between differential proteins and the KEGG pathway, PPI network plots were selected and are shown in Figure 7(e).

Proteomics analysis provided a comprehensive description of protein changes in OPD- and OPD'-treated erythrocytes, but it did not specify the targets for the next step. Differential protein analysis suggested that hemolysis caused by OPD and OPD' may contribute to lipid metabolic disorders (e.g., Q5M872 [41] and Q5XIT9), mitochondrial energy metabolism (e.g., D3ZAQ0 [42] and Q03344), high mobility group protein binding (e.g., P63159 and Q4KLJ0 [43]) and cytoskeletal (e.g., Q6IFU7 [44, 45], Q6IFU9, and A0A0G2JST3). These proteins are very valuable research objects.

3.6. Some Potential Targets Related to Hemolysis Reveal the Difference in Hemolytic Behavior between OPD and OPD'. We first built the three-dimensional molecular structures of OPD and OPD' (see Figure 8) and predicted the putative targets based on the SEA approach and shape-based approach, respectively.

The putative targets of OPD and OPD' predicted by the SEA method are shown in Table 1. Among the 12 targets, the target predicted by the OPD' structure accounted for 100%, while the target predicted by the OPD structure only accounted for 5/12. These 5 targets are indexed as 2, 6, 8, 9, and 10, respectively.

The top 10 targets predicted by the shape similarity method are shown in Table 2.

The putative targets predicted by the shape similarity method were combined with all the putative targets predicted by SEA. These putative targets were then compared with the collected hemolysis-related targets (see Table S1). The results illustrate that the target "solute carrier organic anion transporter family member 1B3" (Q9NPD5) is the potential target for OPD'. Q9NPD5 was submitted to the Reactome Pathway Database for pathway analysis. Detailed pathway information is shown in Table 3.

Q9NPD5, also known as OATP1B3, is an anion transporter. It has been proven that the hepatic uptake of OPD and OPD' is mediated by organic anion-transporting polypeptides (OATPs) [46–48]. This report, on the one hand, confirmed the reliability of the molecular modeling results; on the other hand, it pointed out that OPD and OPD' can affect the transporting activities of OATP1B1 and OATP1B3 in a substrate-dependent manner. Several reports in the literature have shown that the inhibition of organic anion transporting polypeptides OATP1B1 and OATP1B3 might lead to hyperbilirubinemia [49, 50]. This may be one of the reasons why OPD and OPD' cause hemolysis *in vivo*, and it is also a potential hemolysis prevention target worthy of further study.

In addition to Q9NPD5, several other targets that are not directly related to hemolysis are also worthy of attention, such as AT1A1 (Table 1, Index 2), which affects Na⁺-K⁺-ATPase activity, and its effect on hemolysis has been discussed in the previous paragraph. DHCR7 (Table 1,

TABLE 1: The putative targets which predicted by SEA.

Index	Affinity threshold (nM)	<i>p</i> value	Target name	Target description
1	5	5.25E-21	AMYP_HUMAN	Pancreatic alpha-amylase
2	5	1.60E-28	AT1A1_CANLF	Sodium/potassium-transporting ATPase subunit alpha-1
3	5	1.00E-36	CP125_MYCTU	Steroid C26-monooxygenase
4	5	2.85E-09	CP17A_HUMAN	Steroid 17-alpha-hydroxylase/17,20 lyase
5	5	4.51E-06	CP17A_RAT	Steroid 17-alpha-hydroxylase/17,20 lyase
6	5	9.68E-10	DHCR7_RAT	7-Dehydrocholesterol reductase
7	5	3.91E-06	DPOLA_HUMAN	DNA polymerase alpha catalytic subunit
8	5	8.23E-06	EBP_HUMAN	3-Beta-hydroxysteroid-delta(8), delta(7)-isomerase
9	5	1.66E-07	ERG2_YEAST	C-8 sterol isomerase
10	5	7.00E-13	IL2_HUMAN	Interleukin-2
11	5	2.46E-08	MRP4_HUMAN	Multidrug resistance-associated protein 4
12	5	6.15E-29	NPC1_HUMAN	Niemann-Pick C1 protein

TABLE 2: The top 10 predicted targets based on the shape similarity method.

Rank	Entry	Target name	Organism
1	Q11201	CMP-N-acetylneuraminase-beta-galactosamide-alpha-2,3-sialyltransferase 1	Homo sapiens
2	O54939	Testosterone 17-beta-dehydrogenase 3	Rattus
3	Q9UHC9	Niemann-Pick C1-like protein 1	Homo sapiens
4	Q9NPD5	Solute carrier organic anion transporter family member 1B3	Homo sapiens
5	P60568	Interleukin-2	Homo sapiens
6	P08069	Insulin-like growth factor I receptor	Homo sapiens
7	P31749	Serine/threonine-protein kinase AKT	Homo sapiens
8	P04626	Receptor protein-tyrosine kinase erbB-2	Homo sapiens
9	P30304	Dual specificity phosphatase Cdc25A	Homo sapiens
10	P35372	Mu opioid receptor	Homo sapiens

TABLE 3: The pathways details of the target Q9NPD5.

Index	Function	Term
1	Metabolism (Homo sapiens)	Recycling of bile acids and salts
2	Transport of small molecules (Homo sapiens)	Transport of organic anions

Index 6), EBP (Table 1, Index 8), and ERG2 (Table 1, Index 9) proteins encoded by these genes were all involved in the cholesterol biosynthetic pathway, which is part of steroid biosynthesis [51–53]. The interaction between OPD or OPD' and these proteins will further affect the integrity of the cell membrane structure, which may lead to hemolysis. The target predicted by molecular modeling also has limitations, but it provides some references for the study of the potential mechanism of OPD and OPD' hemolysis.

4. Conclusions

In summary, we reported the hemolytic properties of OPD and OPD' and clarified their differences with regard to their hemolytic behavior *in vivo* and *in vitro*. *In vitro*, we established that hemolysis induced by OPD' was related to a redox

imbalance, and OPD has a certain protective effect. We also put forward some reasonable suggestions for safe clinical use. *In vivo*, we confirmed that both OPD and OPD' caused hemolysis, and in addition to redox imbalance, proteomics data revealed that lipid metabolic disorder and mitochondrial energy metabolism have extensive participation in hemolysis. Proteomics and molecular modeling provided a comprehensive description of hemolysis-related protein changes and targets, which may benefit further study of the hemolysis mechanisms of OPD and OPD'.

Data Availability

All data used to support the findings of this study are available from the corresponding author upon request.

Conflicts of Interest

The authors declare that there is no conflict of interest regarding the publication of this paper.

Acknowledgments

The authors would like to thank Xiang-Tao Luo for supporting animal experiments. This research was funded by the National Natural Science Foundation of China (81703669) and National Science and Technology Major Project of “Major New Drug Creation” (2017ZX09301012-007).

Supplementary Materials

See Table S1 in the Supplementary Material for hemolysis-related targets. See Method S1 in the Supplementary Material for detailed proteome analysis conditions. (*Supplementary Materials*)

References

- [1] G. Jacobasch and S. M. Rapoport, “Hemolytic anemias due to erythrocyte enzyme deficiencies,” *Molecular Aspects of Medicine*, vol. 17, no. 2, pp. 143–170, 1996.
- [2] D. Bossi and M. Russo, “Chapter 4 hemolytic anemias due to disorders of red cell membrane skeleton,” *Molecular Aspects of Medicine*, vol. 17, no. 2, pp. 171–188, 1996.
- [3] B. Devalet, F. Mullier, B. Chatelain, J. M. Dogné, and C. Chatelain, “Pathophysiology, diagnosis, and treatment of paroxysmal nocturnal hemoglobinuria: a review,” *European Journal of Haematology*, vol. 95, no. 3, pp. 190–198, 2015.
- [4] W. Barcellini, “Immune hemolysis: diagnosis and treatment recommendations,” *Seminars in Hematology*, vol. 52, no. 4, pp. 304–312, 2015.
- [5] P. Beris and V. Picard, “Non-immune hemolysis: diagnostic considerations,” *Seminars in Hematology*, vol. 52, no. 4, pp. 287–303, 2015.
- [6] E. Fibach and M. Dana, *Red blood cells as redox modulators in hemolytic anemia, Erythrocyte(book)*, intechopen, 2019.
- [7] C. R. Morris, J. H. Suh, W. Hagar et al., “Erythrocyte glutamine depletion, altered redox environment, and pulmonary hypertension in sickle cell disease,” *Blood*, vol. 111, no. 1, pp. 402–410, 2008.
- [8] X. Zhang, G. Campreciós, P. Rimmelé et al., “FOXO3-mTOR metabolic cooperation in the regulation of erythroid cell maturation and homeostasis,” *American Journal of Hematology*, vol. 89, no. 10, pp. 954–963, 2014.
- [9] M. H. Chen, X. J. Chen, M. Wang, L. G. Lin, and Y. T. Wang, “Ophiopogon japonicus—a phytochemical, ethnomedicinal and pharmacological review,” *Journal of Ethnopharmacology*, vol. 181, pp. 193–213, 2016.
- [10] E. Luo, D. Zhang, H. Luo et al., “Treatment efficacy analysis of traditional Chinese medicine for novel coronavirus pneumonia (COVID-19): an empirical study from Wuhan, Hubei Province, China,” *China Chinese Medicine*, vol. 15, no. 1, p. 34, 2020.
- [11] H.-Y. Wang, S.-C. Guo, Z.-T. Peng et al., “Ophiopogon polysaccharide promotes the in vitro metabolism of ophiopogonins by human gut microbiota,” *Molecules*, vol. 24, no. 16, p. 2886, 2019.
- [12] A. Q. Jin, G. Yang, M. Chen et al., “Analysis and evaluation of nutrient composition of Ophiopogonis Radix in Santai area,” *Zhongguo Zhong Yao Za Zhi*, vol. 44, no. 15, pp. 3226–3232, 2019.
- [13] Y.-Y. Zhang, C. Meng, X.-M. Zhang et al., “Ophiopogonin D attenuates doxorubicin-induced autophagic cell death by relieving mitochondrial damage in vitro and in vivo,” *The Journal of Pharmacology and Experimental Therapeutics*, vol. 352, no. 1, pp. 166–174, 2014.
- [14] X. Huang, Y. Wang, Z. Zhang et al., “Ophiopogonin D and EETs ameliorate Ang II-induced inflammatory responses via activating PPAR α in HUVECs,” *Biochemical and Biophysical Research Communications*, vol. 490, no. 2, pp. 123–133, 2017.
- [15] J. H. Lee, C. Kim, and S. G. Lee, “Ophiopogonin D, a steroidal glycoside abrogates STAT3 signaling cascade and exhibits anti-cancer activity by causing GSH/GSSG imbalance in lung carcinoma,” *Cancers*, vol. 10, no. 11, p. 427, 2018.
- [16] J. Qian, F. Jiang, B. Wang et al., “Ophiopogonin D prevents H₂O₂-induced injury in primary human umbilical vein endothelial cells,” *Journal of Ethnopharmacology*, vol. 128, 2010.
- [17] J. Wang, N. N. Wang, Y. X. Ge et al., “Ophiopogonin D protects cardiomyocytes against ophiopogonin D'-induced injury through suppressing endoplasmic reticulum stress,” *Zhongguo Zhong Yao Za Zhi*, vol. 44, no. 9, pp. 1876–1881, 2019.
- [18] S. Ren, X. U. Huanhua, L. I. Ming et al., “Cytotoxicity of ophiopogonin D' for rat H9c2 cardiomyocytes,” *Chinese Journal of Pharmacology and Toxicology*, vol. 31, no. 4, pp. 325–331, 2017.
- [19] Z. Lu, H. Wang, M. Zhu et al., “Ophiopogonin D', a natural product from Radix Ophiopogonis, induces in vitro and in vivo RIPK1-dependent and caspase-independent apoptotic death in androgen-independent human prostate cancer cells,” *Frontiers in Pharmacology*, vol. 9, 2018.
- [20] Z. Lu, C. Wu, M. Zhu et al., “Ophiopogonin D' induces RIPK1-dependent necroptosis in androgen-dependent LNCaP prostate cancer cells,” *International Journal of Oncology*, vol. 56, no. 2, 2020.
- [21] A. Zha, Z. Cui, M. Qi et al., “Dietary baicalin zinc supplementation alleviates oxidative stress and enhances nutrition absorption in deoxynivalenol challenged pigs,” *Current Drug Metabolism*, vol. 10, no. 8, pp. 2174–2625, 2020.
- [22] P. Liao, Y. Li, M. Li et al., “Baicalin alleviates deoxynivalenol-induced intestinal inflammation and oxidative stress damage by inhibiting NF- κ B and increasing mTOR signaling pathways in piglets,” *Food and Chemical Toxicology*, vol. 140, p. 111326, 2020.
- [23] I. Baranowska and S. Bajkacz, “A new UHPLC-MS/MS method for the determination of flavonoids in supplements and DPPH-UHPLC-UV method for the evaluation of the radical scavenging activity of flavonoids,” *Food Chemistry*, vol. 256, pp. 333–341, 2018.
- [24] A. Zha, D. Yuan, Z. Cui et al., “The evaluation of the antioxidant and intestinal protective effects of baicalin-copper in deoxynivalenol-challenged piglets,” *Oxidative Medicine and Cellular Longevity*, vol. 2020, 13 pages, 2020.
- [25] Y. Wu, F. Wang, L. Fan et al., “Baicalin alleviates atherosclerosis by relieving oxidative stress and inflammatory responses via inactivating the NF- κ B and p38 MAPK signaling pathways,” *Biomedicine & Pharmacotherapy*, vol. 97, pp. 1673–1679, 2018.

- [26] S. Wang, G. L. Dale, P. Song, B. Viollet, and M. H. Zou, "AMP-Kalpa1 deletion shortens erythrocyte life span in mice: role of oxidative stress," *The Journal of Biological Chemistry*, vol. 285, no. 26, pp. 19976–19985, 2010.
- [27] S. Wang, G. L. Dale, P. Song, B. Viollet, and M. H. Zou, "Correction: AMPK α 1 deletion shortens erythrocyte life span in mice: role of oxidative stress," *The Journal of Biological Chemistry*, vol. 294, no. 27, p. 10738, 2019.
- [28] J. R. Wiśniewski, A. Zougman, N. Nagaraj, and M. Mann, "Universal sample preparation method for proteome analysis," *Nature Methods*, vol. 6, no. 5, pp. 359–362, 2009.
- [29] Q. Wu, Y. Li, Y. Wang, and H. Lu, "Quantitative mass spectrometry imaging of amino acids with isomer differentiation in brain tissue via exhaustive liquid microjunction surface sampling-tandem mass tags labeling-ultra performance liquid chromatography-mass spectrometry," *Journal of Chromatography. A*, vol. 1621, p. 461086, 2020.
- [30] M. J. Keiser, B. L. Roth, B. N. Armbruster, P. Ernsberger, J. J. Irwin, and B. K. Shoichet, "Relating protein pharmacology by ligand chemistry," *Nature Biotechnology*, vol. 25, no. 2, pp. 197–206, 2007.
- [31] P. Ding, X. Yan, Z. Liu et al., "PTS: a pharmaceutical target seeker," *Database*, vol. 2017, 2017.
- [32] X. Yan, J. Li, Z. Liu, M. Zheng, H. Ge, and J. Xu, "Enhancing molecular shape comparison by weighted Gaussian functions," *Journal of Chemical Information and Modeling*, vol. 53, no. 8, pp. 1967–1978, 2013.
- [33] Z. Feng and H. Wang, "Enzymatic assemblies disrupt the membrane and target endoplasmic reticulum for selective cancer cell death," *Journal of the American Chemical Society*, vol. 140, no. 30, pp. 9566–9573, 2018.
- [34] M. Yang, Y. Li, J. S. Ye, Y. Long, and H. M. Qin, "Effect of PFOA on oxidative stress and membrane damage of *Escherichia coli*," *Huan Jing Ke Xue*, vol. 38, no. 3, pp. 1167–1172, 2017.
- [35] P. C. N. Biapa, H. Matei, Ş. Bălci, J. E. Oben, and J. Y. Ngogang, "Protective effects of stem bark of *Harungana madagascariensis* on the red blood cell membrane," *BMC Complementary and Alternative Medicine*, vol. 13, no. 1, p. 98, 2013.
- [36] A. E. Maciag, R. J. Holland, Y. S. Robert Cheng et al., "Nitric oxide-releasing prodrug triggers cancer cell death through deregulation of cellular redox balance," *Redox Biology*, vol. 1, no. 1, pp. 115–124, 2013.
- [37] P. Iiu, O. V. Simonenko, K. M. Burnysheva et al., "The ability of cells to adjust to the low oxygen content associated with Na,K-ATPase glutathionylation," *Molekuliarnaia Biologiia*, vol. 49, no. 1, pp. 175–183, 2015.
- [38] X. Huan-Hua, Z. H. Jiang, C. S. Huang et al., "Established UPLC-MS / MS method to determinate ophiopogonin D and ophiopogonin D' and clinical risk assessment," *Drug Evaluation Research*, vol. 42, no. 6, pp. 1135–1140, 2019.
- [39] T. Kamesaki, "Diagnosis and treatment of hemolytic anemia," *Rinshō Ketsueki*, vol. 56, no. 10, pp. 1894–1902, 2015.
- [40] H. D. Zhang, Y. J. Ma, Q. F. Liu et al., "Human erythrocyte life-span measured by Levitt's CO breath test with newly developed automatic instrument," *Journal of Breath Research*, vol. 12, no. 3, article 036003, 2018.
- [41] D. E. Moller, "New drug targets for type 2 diabetes and the metabolic syndrome," *Nature*, vol. 414, no. 6865, pp. 821–827, 2001.
- [42] T. M. Decker, I. Forné, T. Straub et al., "Analog-sensitive cell line identifies cellular substrates of CDK9," *Oncotarget*, vol. 10, no. 65, pp. 6934–6943, 2019.
- [43] X. L. Gao, W. J. Tian, B. Liu, J. Wu, W. Xie, and Q. Shen, "High-mobility group nucleosomal binding domain 2 protects against microcephaly by maintaining global chromatin accessibility during corticogenesis," *Journal of Biological Chemistry*, vol. 295, no. 2, pp. 468–480, 2020.
- [44] D. A. Fletcher and R. D. Mullins, "Cell mechanics and the cytoskeleton," *Nature*, vol. 463, no. 7280, pp. 7485–7492, 2010.
- [45] T. Hohmann and F. Dehghani, "The cytoskeleton-a complex interacting meshwork," *Cell*, vol. 8, no. 4, p. 362, 2019.
- [46] X. Liu, L. Chen, M. Liu et al., "Ginsenoside Rb1 and Rd remarkably inhibited the hepatic uptake of Ophiopogonin D in Shenmai injection mediated by OATPs/oatps," *Frontiers in Pharmacology*, vol. 9, p. 957, 2018.
- [47] W. Zhang, X. Xiong, L. Chen et al., "Hepatic uptake mechanism of Ophiopogonin D mediated by organic anion transporting polypeptides," *European Journal of Drug Metabolism and Pharmacokinetics*, vol. 42, no. 4, pp. 669–676, 2017.
- [48] L. Chen, L. Liu, Y. Chen et al., "Modulation of transporter activity of OATP1B1 and OATP1B3 by the major active components of *Radix Ophiopogonis*," *Xenobiotica*, vol. 49, no. 10, pp. 1221–1228, 2019.
- [49] E. Kotsampasakou, S. E. Escher, and G. F. Ecker, "Linking organic anion transporting polypeptide 1B1 and 1B3 (OATP1B1 and OATP1B3) interaction profiles to hepatotoxicity - the hyperbilirubinemia use case," *European Journal of Pharmaceutical Sciences*, vol. 100, pp. 9–16, 2017.
- [50] E. van de Steeg, V. Stránecký, H. Hartmannová et al., "Complete OATP1B1 and OATP1B3 deficiency causes human rotor syndrome by interrupting conjugated bilirubin reuptake into the liver," *The Journal of Clinical Investigation*, vol. 122, no. 2, pp. 519–528, 2012.
- [51] S. Silve, P. H. Dupuy, C. Labit-Lebouteiller et al., "Emopamil-binding protein, a mammalian protein that binds a series of structurally diverse neuroprotective agents, exhibits $\Delta 8$ - $\Delta 7$ sterol isomerase activity in yeast," *The Journal of Biological Chemistry*, vol. 271, no. 37, pp. 22434–22440, 1996.
- [52] F. F. Moebius, K. E. M. Soellner, B. Fiechtner, C. W. Huck, G. Bonn, and H. Glossmann, "Histidine77, glutamic acid81, glutamic acid123, threonine126, asparagine194, and tryptophan197 of the human emopamil binding protein are required for in vivo sterol delta 8-delta 7 isomerization," *Biochemistry*, vol. 38, no. 3, pp. 1119–1127, 1999.
- [53] F. F. Moebius, B. U. Fitzky, G. Wietzorrek, A. Haidekker, A. Eder, and H. Glossmann, "Cloning of an emopamil-binding protein (EBP)-like protein that lacks sterol delta8-delta7 isomerase activity," *The Biochemical Journal*, vol. 374, no. 1, pp. 229–237, 2003.